doi:10.1038/nature12149

CGE analysis

In the standard GCR assay, expression of both *CAN1* and *URA3* must be lost to generate clones that will grow on plates containing 5-FOA and canavanine (FOA+Can). After standard GCR events, these genes are not expressed because they are physically lost by *de novo* telomere addition or non-reciprocal translocation or large deletion. However, PCR and Southern analysis demonstrated that telomere addition was not common, and *URA3* and *CAN1* were present at their original locations in many *pif1-m2* + G4 and *pif1-m2 rrm3*Δ + G4 (and some *pif1-m2 rrm3*Δ) clones. To determine if genes were mutated, the genes and ~200 bp of their up- and downstream flanking sequences were cloned and sequenced. Similar analyses of 11 independent *sgs1*Δ + G4 GCR clones showed that *CAN1* and *URA3* were missing (data not shown), suggesting that the *pif1-m2* + G4, *pif1-m2 rrm3*Δ + G4, and *pif1-m2 rrm3*Δ silencing of *CAN1* and *URA3* is enhanced by lack of nuclear Pif1 function and a nearby G4 motif. To investigate this phenomenon in more detail, we tested all of the markers (*URA3*, *CAN1*, and *LEU2*, which marks the G4 motif) in the parental GCR strains and found that the WT, *pif1-m2*, *sgs1*Δ, and *pif1-m2 rrm3*Δ strains all grew on –Ura medium (and those with the G4 insert grew on –Leu medium) but not on media containing FOA, Can, or both (data not shown). Thus, before the GCR assay, all of the markers functioned as expected. Similar plating assays with the post-GCR *pif1-m2* + G4, *pif1-m2 rrm3*Δ + G4, and *pif1-m2 rrm3*Δ clones demonstrated that they grew on FOA, Can, and FOA+Can plates, as well as on –Ura (data not shown), despite the presence of WT *URA3* and *CAN1*. Together, the above data suggest that either transcription or translation of *URA3* is silenced, and this silencing is somehow related to lack of nuclear Pif1 and the presence of the G4 insert. As a control for this hypothesis, we characterized the rare GCR events that occur in the *pif1-m2* "no insert" strain that were not due to telomere addition and found that the *CAN1* and *URA3* markers were missing, not silenced.

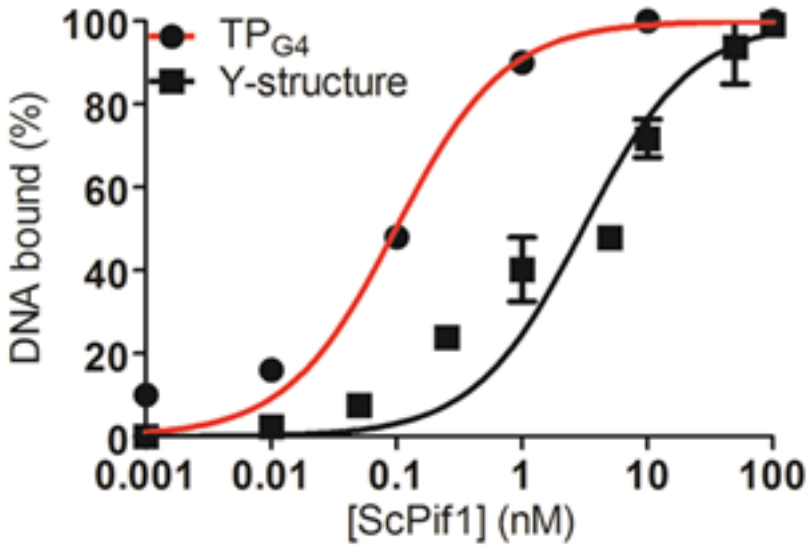

Supplementary Figure 1. Binding of the TP_{G4} and Y-structure substrates (0.1 nM) as a function of [ScPif1]. Error bars here and in all subsequent figures correspond to one standard deviation of the mean from ≥3 independent experiments.

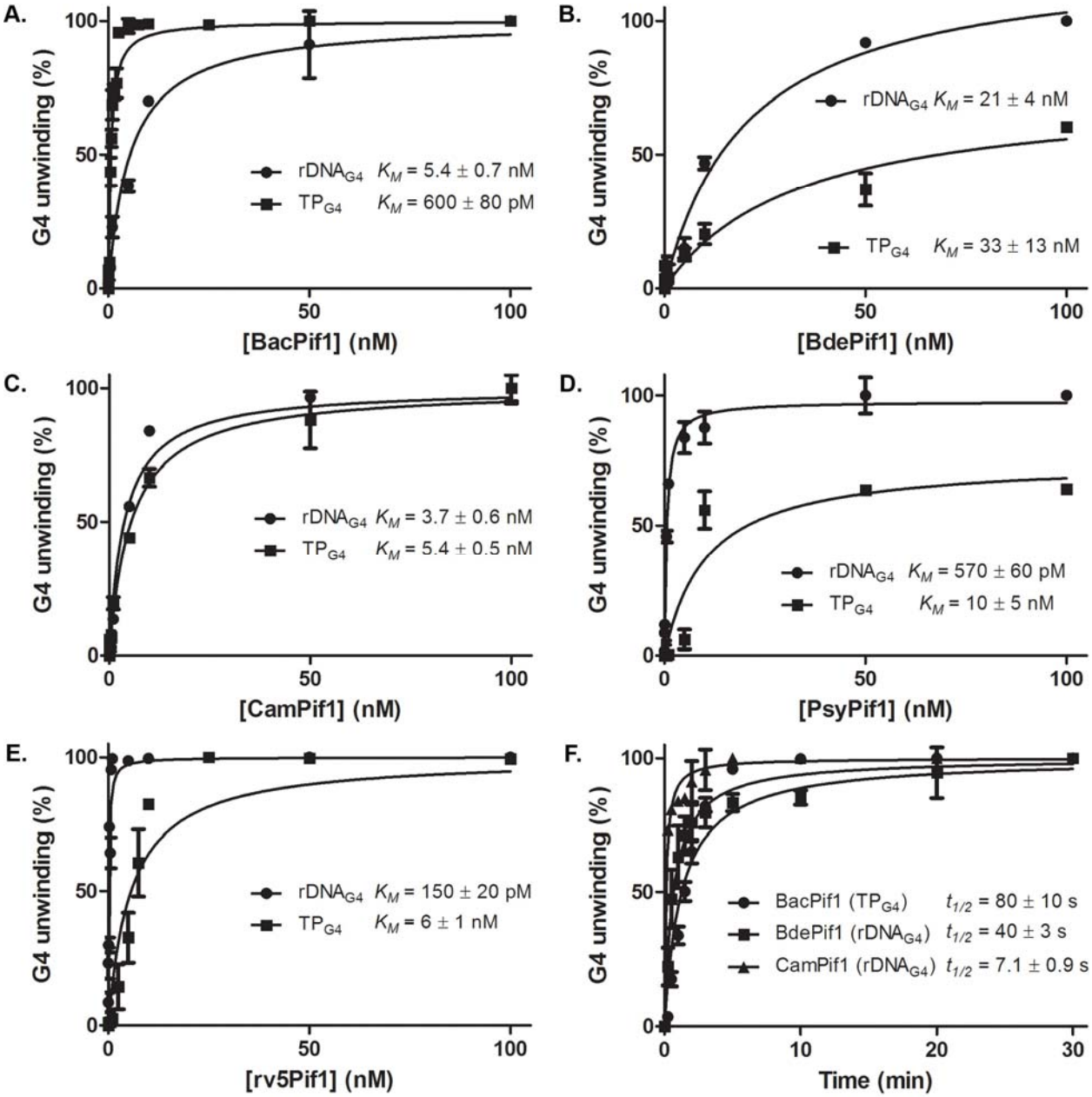

Supplementary Figure 2. Prokaryotic Pif1 G4 DNA helicase assays. Unwinding of the rDNA$_{G4}$ and TP$_{G4}$ substrates (0.1 nM) as a function of the concentration of (a) BacPif1, (b) BdePif1, (c) CamPif1, (d) PsyPif1, and (e) rv5Pif1. The apparent K_Ms represent the midpoints of the protein titration curves. (f) Time course analyses of G4 DNA unwinding by the BacPif1, BdePif1, and CamPif1 helicases. The rates of BacPif1, BdePif1, and CamPif1 G4 unwinding are 38, 75, and 420 pM G4/min.

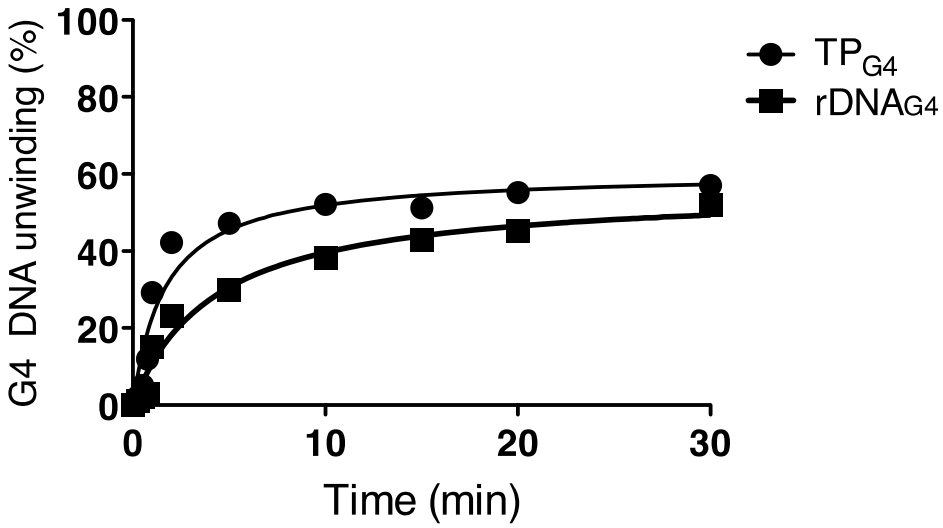

Supplementary Figure 3. hWRN G4 DNA helicase assays. Time course of the unwinding of the TP_{G4} and $rDNA_{G4}$ substrates (100 pM) by 100 nM hWRN at 37°C. There are no error bars because the data are the average of two independent experiments.

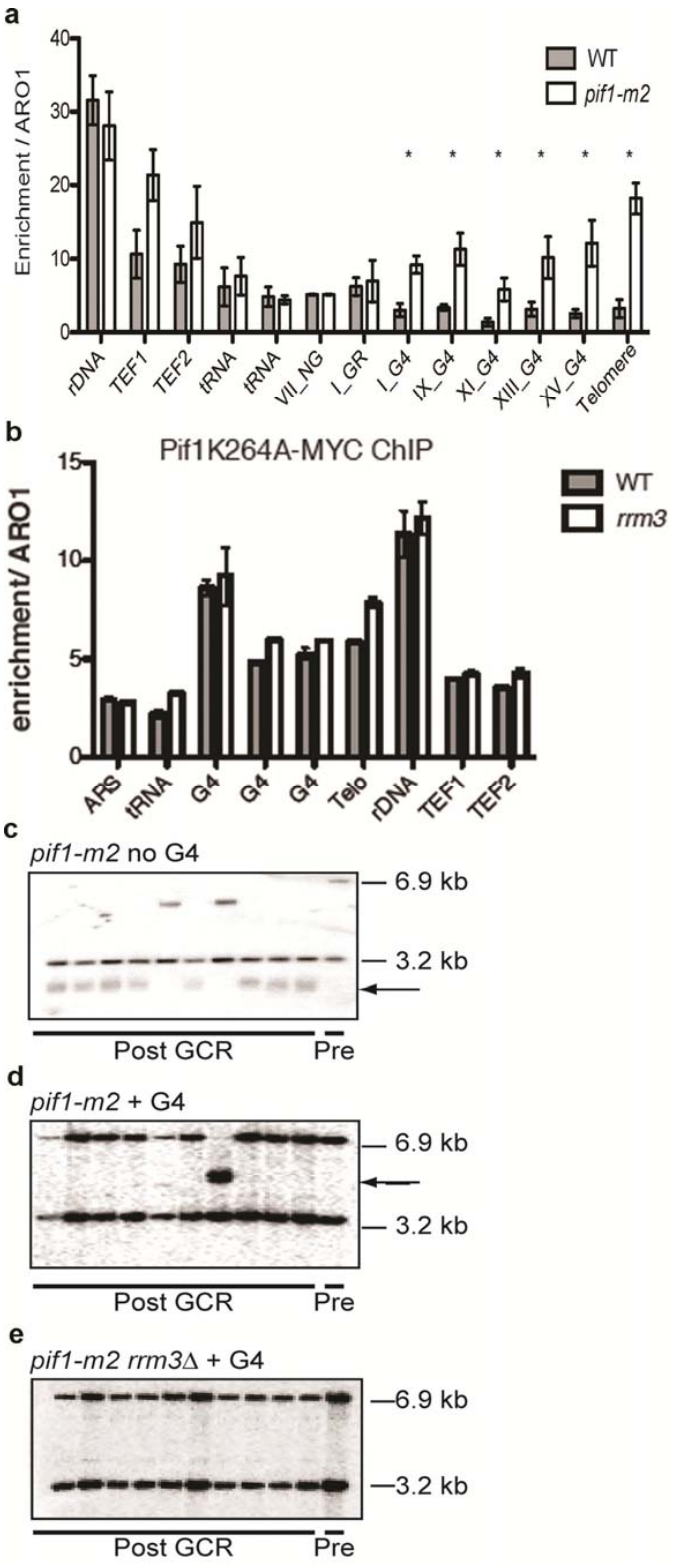

Supplementary Figure 4. Increased Rrm3 binding to G4 motifs in the absence of ScPif1 and types of GCR events. (**a**) Rrm3-Myc binding to five G4 motifs and eight non-G4 motifs in WT (gray) and *pif1-m2* (white) cells. Binding was normalized to input DNA and *ARO1*. * indicates a

statistically significant difference (p<0.0014) in Rrm3 binding in *pif1-m2* vs. WT cells as calculated by the Student's *t*-test. (**b**) ChIP-qPCR analysis of Pif1-K264A binding in WT (grey bars) and *rrm3*Δ (white bars) cells. Pif1-K264A was C-terminally tagged at its endogenous locus with 13 Myc epitopes as described[19]. Pif1-K264A binding was measured at three candidate G4 motifs, two non-G4 Pif1 binding sites (rDNA; and telomere VI-R, Telo), and four Rrm3-dependent sites (tRNA, *ARS*, *TEF1*, and *TEF2*) (Rrm3 dependent sites are places where replication pauses in the absence of Rrm3[18]). Values were normalized to both input and the amount of *ARO1* DNA in the immunoprecipitate and are not significantly different by the Student's *t*-test. (**c-e**) Southern blot analyses of *Alw*NI-digested DNA from independent GCR clones from (**c**) *pif1-m2*, (**d**) *pif1-m2*+G4, and (**e**) *pif1-m2 rrm3*Δ+G4 cells. Blots were digested with *Alw*NI and probed with *CIN8* (primer pair 3 from A). In d, e, and f, 8/10, 1/10, and 0/10 clones display apparent telomere additions ("fuzzy" bands, arrow). See Supplementary Information for an explanation of the banding pattern. The banding pattern for the *pif1-m2 rrm3*Δ clones containing no G4 insert looks similar to f (data not shown), but the silencing phenotype of the cells is not the same. The lack of telomere addition in the *pif1-m2 rrm3*Δ strains with or without a G4 insert is consistent with the previous finding that *rrm3*Δ suppresses *pif1* telomere addition[26].

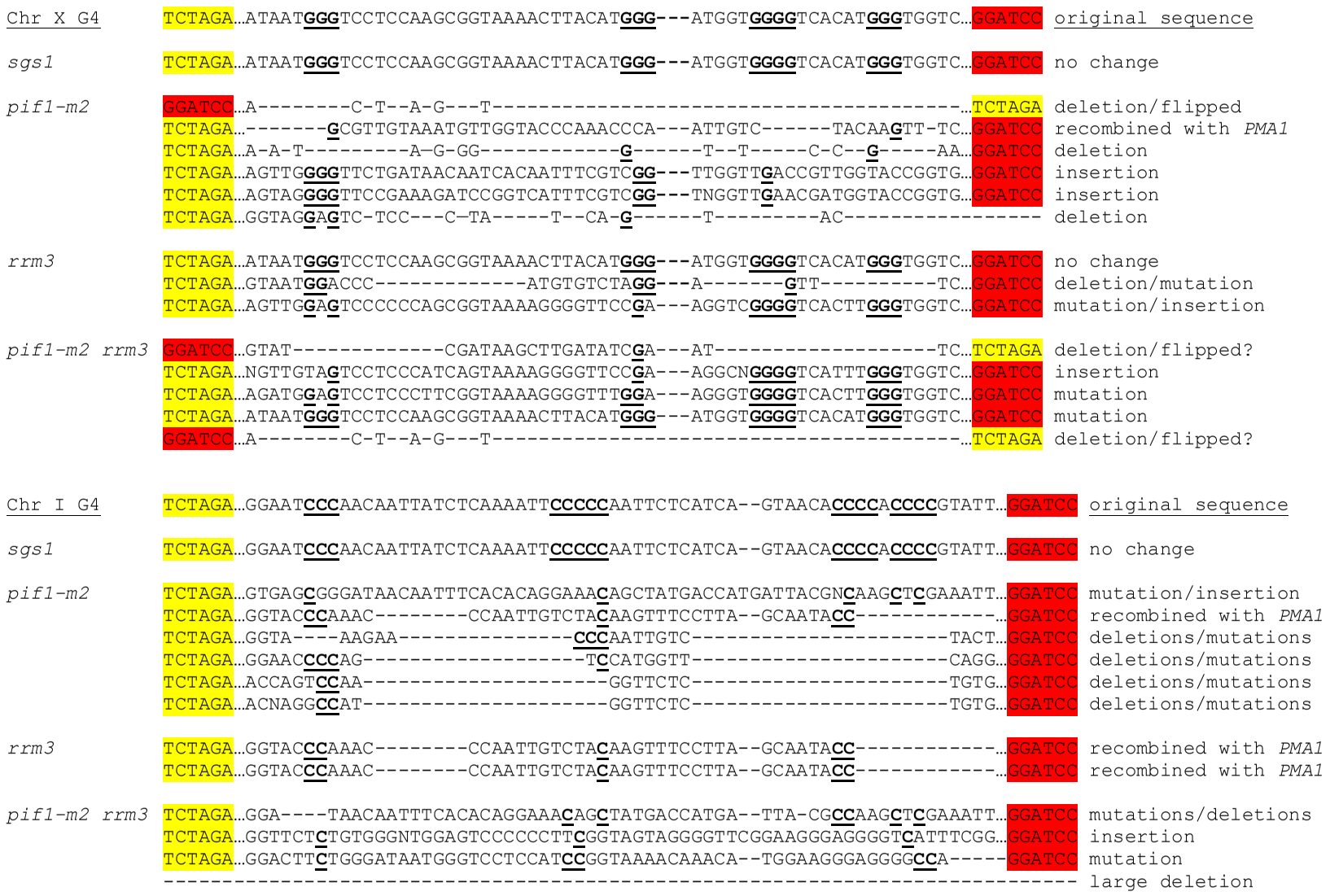

Supplementary Figure 5. Sequences of G4 inserts in representative GCR clones. ClustalW alignment of the G4 insert sequences after GCR assays in the strains indicated on the left relative to the original Chr I_{G4} and Chr X_{G4} sequences (underlined on left). The *Xba*I and *Bam*HI sites used to clone the inserts into pRS415 (Supplementary Table 8) are highlighted in yellow and red, respectively; this

~200 bp region is within the ~1 kb region that was amplified by PCR prior to sequencing. The ellipses represent endogenous flanking sequences that were PCR amplified with the G4 motifs from *S. cerevisiae* genomic DNA, which was omitted to simply presentation of the data. The types of post-GCR alterations noted in the G4 motifs extended into these flanking sequences. The G4 motif begins and ends at the first and last underlined residues, respectively, in the Chr I_{G4} and Chr X_{G4} sequences. In the original motifs, the underlined residues are predicted to participate in G-G base pairing to form the G4 structure; the Chr I_{G4} forms on the complementary strand. In the mutated sequences, the underlined residues are no longer predicted to form G4 structures. The type of event that occurred at the G4 motif (*e.g.,* deletion or mutation) is indicated on the right. In the GCR clones, dashes represent deleted residues. In the original Chr I_{G4} and Chr X_{G4} sequences, dashes represent sites of insertions in one or more GCR clones.

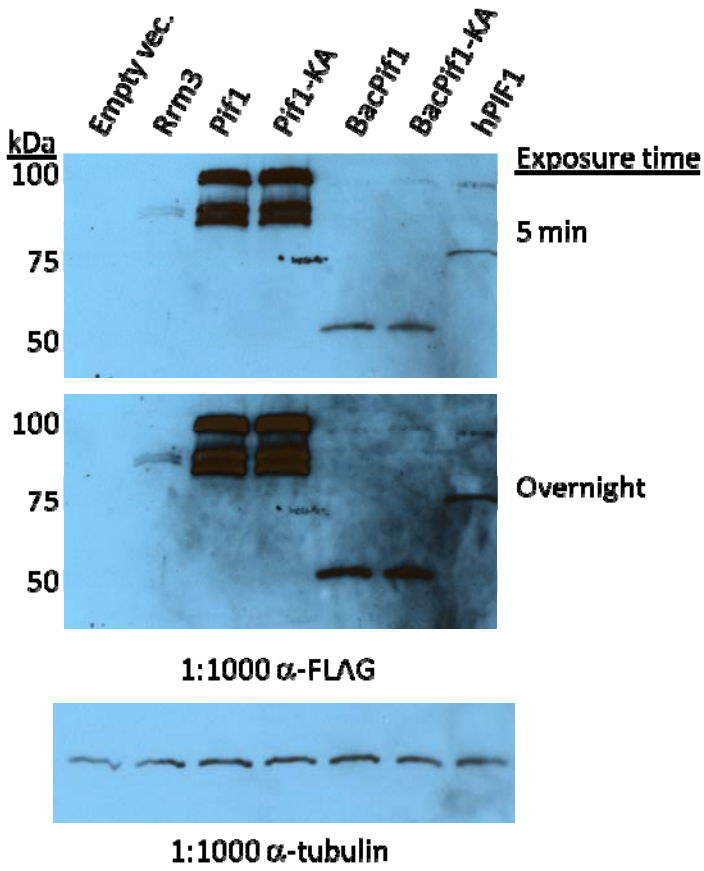

Supplementary Figure 6. Helicase expression in the *pif1-m2 rrm3*Δ + X_{G4} strains. The various helicases were C-terminally tagged with 3xFLAG and expressed from a *TRP1*-marked *CEN* vector under the control of the *RRM3* promoter. Whole cell extracts were prepared, proteins were separated on an 8% polyacrylamide gel, transferred to nitrocellulose, and probed with an anti-FLAG antibody. The blot was then stripped and re-probed with an anti-tubulin antibody as a loading control. The expected molecular weights of the recombinant proteins are indicated. Three bands appear in the ScPif1 and ScPif1-KA lanes; the two lower molecular weight bands are likely degradation products from proteolysis of the N-terminus. Expected molecular weights: Rrm3, 84 kDa; Pif1 and Pif1-KA, 100 kDa; BacPif1 and BacPif1-KA, 52 kDa; and hPIF1, 75 kDa.

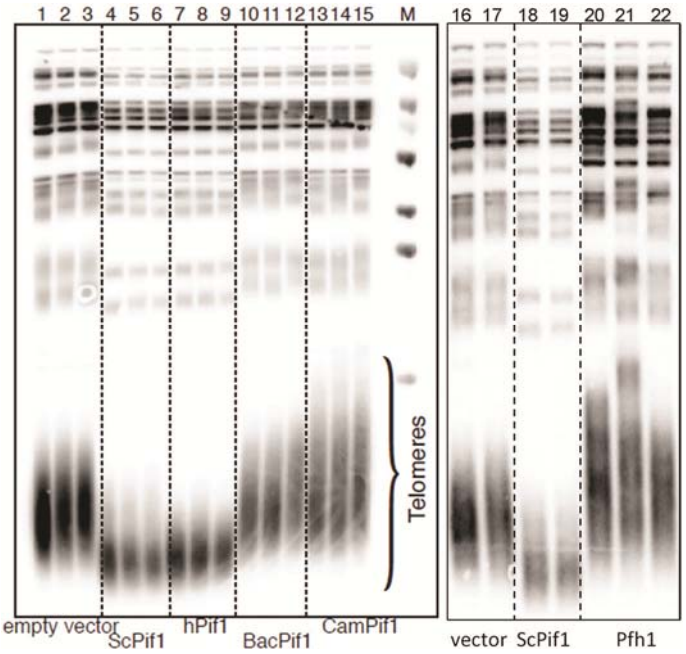

Supplementary Figure 7. Telomere length in *pif1-m2* cells heterologously expressing Pif1 family helicases. Full blot image of Southerns shown in Figure 5c.

Table S1. Helicases tested for G4 DNA binding and unwinding.

Enzyme	Species	Type (polarity)	Protein length	G4 binding	G4 unwinding	Reference(s)
ATRX	Human	DNA (N.D.)	Full length	Yes	N.D.[1]	[21]
BLM	Human	DNA (3'-5')	Full length	Yes (2.8)[2]	Yes	[22-25]
ChlR1/DDX11	Human	DNA (5'-3')	Full length	Yes (~2-8)	Yes[3]	[26]
DHX9/NDH II/RHA	Human	RNA (3'-5')	Full length	N.D.	Yes	[27]
DnaB	*E. coli*	DNA (5'-3')	Full length	N.D.	Yes	M. Bochman, unpublished results
Dna2	*S. cerevisiae*	DNA (5'-3')	Not described	Yes	Yes	[28]
hDna2	Human	DNA (5'-3')	Not described	Yes (~6)	Yes	[28]
DNA helicase IV/nucleolin	Human	Both (5'-3')	284-709/710[4]	Yes (≥79)	N.D.[5]	[29]
FANCJ	Human	DNA (5'-3')	Full length	N.D.	Yes (~1-2)	[30]
gp41	phage T4	DNA (5'-3')	Full length	N.D.	Yes	M. Bochman, unpublished results

[1] N.D. = not determined.
[2] The numbers in parentheses indicate the K_d (G4 binding) or K_M (G4 unwinding) in nM.
[3] Preferentially unwinds two-stranded antiparallel G2' G4 substrate relative to four-stranded parallel G4 substrate.
[4] Indicates the amino acids comprising the truncated polypeptide/total amino acids in the full-length protein.
[5] Hypothesized to induce G4 formation.

LTAg	SV40	DNA (3'-5')	Full length	N.D.	Yes	[31, 32]
Pif1	*S. cerevisiae*	DNA (5'-3')	Full length[6]	Yes (~0.07-0.14)	Yes (~0.01)	[33] Current manuscript
hPIF1	Human	DNA (5'-3')	Full length[6]	Yes	Yes	[34]
RecBCD	*E. coli*	DNA (bi-polar)	Full length	N.D.	No[7]	[23]
RecQ	*E. coli*	DNA (3'-5')	Full length	N.D.	Yes	[35]
RecQ1	Human	DNA (3'-5')	57-649/649	Yes (1.8)	No[8]	[24]
RHAU/DHX36/G4R1	Human	RNA	Full length	Yes (low pM) to nM range)	Yes	[36, 37]
RHAU/CG9323	*Drosophila melanogaster*	RNA	Full length	Yes	Yes	[37]
SARS cov helicase	coronavirus	DNA	Full length	Yes	Yes	[38]
Sgs1	*S. cerevisiae*	DNA (3'-5')	Full length	Yes[9]	Yes[10]	Current manuscript
Sgs1 truncation	*S. cerevisiae*	DNA (3'-5')	400-1268/1447	Yes (5)	Yes	[25]
Srs2	*S. cerevisiae*	DNA (3'-5')	1-898/1174	N.D.	Yes	M. Bochman, unpublished results
WRN	Human	DNA (3'-5')	Full length	N.D.	Yes	[22, 27, 39]

[6] Nuclear isoform.
[7] Only tested on one G4 substrate (TP) but unwound forked and partial duplex DNAs under same reaction conditions.
[8] Inactive on G2' and parallel G4 substrates but active on forked and Holliday junction substrates.
[9] Binding is poor to three tested G4 substrates, precluding the accurate determination of a dissociation constant.
[10] G4 DNA unwinding is poor relative to unwinding of a forked DNA substrate.

Table S2. Sequences used in DNA binding and helicases assays.

G4 motif	*S. cerevisiae* chromosome	Sequence (5'-3')
Poly(dA)	N/A	AAAAAAAAAAAAAAAAAAAA
Poly(dC)	N/A	CCCCCCCCCCCCCCCCCCCC
Poly(dG)	N/A	GGGGGGGGGGGGGGGGGGGG
Poly(dT)	N/A	TTTTTTTTTTTTTTTTTTTT
G-rich	N/A	CGGCCCGGCGGTCCGCGGTC
Non G-rich	N/A	CAAAGGACCCTTTGTGGATC
rDNA $_{G4}$	XII	GGGTAACGGGGAATAAGGGTTCGATTCCGGAGAGGG
TP $_{G4}$	N/A	GGGGGAGCTGGGGTAGATGGGAATGTGAGGG
Chr IV $_{G4}$	IV	GGGGAGGGGAAGGGGAGGGG
Chr IX $_{G4}$	IX	GGGTACGGTGGGTAATAAGGGAAGGTATCGGG
Chr X $_{G4}$	X	GGGTCCTCCAAGCGGTAAAACTTACATGGGATGGTGGGGTCACA
Chr XI $_{G4}$	XI	TGGG
Chr XII $_{G4}$	XII	GGGCACGGGCACTCAATGGACGGGGTATCCACCCAGCTTGGAAA GGGG
Y-structure	N/A	GGGGTGGTGCTTCAGCCTGGGGTAACAAATCAAGTTGGGGCGGT GCATCCACTTGGGCGTCGGG Top = TTTTTTTTTTTTTTTTTTTTTTTTTTTTTTGACGCTGCCGAATTCTG GCTTGCT Bottom = TGAGTGAGCAAGCCAGAATTCGGCAGCGTCTTTTTTTTTTTTTTTT TTTTTTTTTTTTT

Tested G4 motifs are from the *S. cerevisiae* genome [10, 19] except G4-TP. G4-TP is a well-characterized four-stranded parallel G4 DNA substrate derived from a mouse immunoglobulin locus [23]. All G4 substrates contained either a 5' or 3' 10-nt poly(dA) tail (not shown) for ScPif1 or Sgs1 experiments, respectively. The Y-structure substrate was prepared by annealing the top and bottom oligonucleotides listed above and filling in the top strand with α^{32}P-dCTP and unlabeled dATP, dGTP, and dTTP using Klenow Fragment (3'→5' exo$^-$) (NEB).

Table S3. Sequences used in GCR assays.

G4 motif	*S. cerevisiae* chromosome	Sequence (5'-3')
I_{G4}	I	CCCAACAATTATCTCAAAATTCCCCCAATTCTCATCAGTAACACC CCACCCC
X_{G4}	X	GGTGGGTAATAAGGGAAGGTATCGGGATTGGGG
NG	VII	CTAATCTTTCAGCGTTGTAAATGTTGGTACCCAAACCCAATTGTC TACAAGTTTCCTTAGC
GR	I	ATGGTGGTCATCTCAGTAGATGTAGAGGTGAAAGTACCGGTCCA TGGCTCGGT

Table S4. Yeast strains

Strain	Genotype	Reference or source
YPH500	*MATα ura3-52 lys2-801 ade2-101 trp1Δ63 his3Δ200 leu2Δ1*	[1]
YPH499	*MATa ura3-52 lys2-801 ade2-101 trp1Δ63 his3Δ200 leu2Δ1*	[1]
KP359	*MATa ura3-52 lys2-801 ade2-101 trp1Δ63 his3Δ200 leu2Δ1 Rrm3-MYC13::TRP1 pif1-m2*	This study
KP349	*MATa ura3-52 lys2-801 ade2-101 trp1Δ63 his3Δ200 leu2Δ1 Rrm3-MYC13::HIS3*	This study
KP448	*MATa/α ura3-52 lys2-801 ade2-101 trp1Δ63 his3Δ200 leu2Δ1 PIF1/pif1-m2*	This study

Table S5. *Saccharomyces cerevisiae* strains used for gross-chromosomal rearrangement assays.

Strain	Gene(s) of interest	Insert	Plasmid
MBY49	WT	No insert	-
KP296	WT	G4-I	-
KP327	WT	G4-X	-
KP298	WT	G-rich	-
KP299	WT	Non-G-rich	-
KP313	*pif1-m2*	No insert	-
KP323	*pif1-m2*	G4-I	-
KP322	*pif1-m2*	G4-X	-
KP330	*pif1-m2*	G-rich	-
KP329	*pif1-m2*	Non-G-rich	-
MBY79	*rrm3*Δ	No insert	-
KP304	*rrm3*Δ	G4-I	-
KP328	*rrm3*Δ	G4-X	-
KP332	*rrm3*Δ	G-rich	-
KP331	*rrm3*Δ	Non-G-rich	-
MBY132	*sgs1*Δ	No insert	-
KP314	*sgs1*Δ	G4-I	-
KP324	*sgs1*Δ	G4-X	-
KP311	*pif1-m2 rrm3*Δ	No insert	-
KP325	*pif1-m2 rrm3*Δ	G4-I	-
KP326	*pif1-m2 rrm3*Δ	G4-X	-
KP334	*pif1-m2 rrm3*Δ	G-rich	-
KP333	*pif1-m2 rrm3*Δ	Non-G-rich	-
KP351	*pif1-m2 sgs1*Δ	No insert	-

KP352	*pif1-m2 sgs1*Δ	G4-I	-
KP353	*pif1-m2 sgs1*Δ	G4-X	-
MBY225	*pif1-m2 rrm3*Δ	G4-X	pMB13 (empty vector)
MBY222	*pif1-m2 rrm3*Δ	G4-X	pMB282 (ScPif1)
MBY223	*pif1-m2 rrm3*Δ	G4-X	pMB283 (ScPif1-KA)
MBY224	*pif1-m2 rrm3*Δ	G4-X	pMB274 (Rrm3)
MBY194	*pif1-m2 rrm3*Δ	G4-X	pMB272 (Pfh1)
MBY233	*pif1-m2 rrm3*Δ	G4-X	pMB292 (hPIF1)
MBY213	*pif1-m2 rrm3*Δ	G4-X	pMB270 (BacPif1)
MBY217	*pif1-m2 rrm3*Δ	G4-X	pMB288 (BacPif1-KA)
MBY252	*pif1-m2 rrm3*Δ	G4-X	pMB267 (BdePif1)
MBY250	*pif1-m2 rrm3*Δ	G4-X	pMB289 (BifPif1)
MBY209	*pif1-m2 rrm3*Δ	G4-X	pMB303 (CamPif1)
MBY251	*pif1-m2 rrm3*Δ	G4-X	pMB304 (V99B1Pif1)
MBY221	*pif1-m2 rrm3*Δ	G4-X	pMB305 (PsyPif1)

*All tested inserts (~200-250 bp) were identified as regions with strong Pif1 binding [19]. G4-I, G4 motif from chromosome I; G4-X, G4 motif from chromosome X; G-rich, G-rich sequence from chromosome I; Non-G-rich, non-G-rich sequence from chromosome VII.

Table S6. Oligonucleotides used for cloning.

A) Oligonucleotides used for gross-chromosomal rearrangement strain construction.

Modification	Oligo	Sequence (5'-3')
hxt13::URA3	MB262	GCACGTAAGGCATAACAATCAAAAAAAGAAAAAAGAAA CAAAAGTTAAACCAAAAAAAAAAACAGCTGAAGCTTCGT ACGC
	MB277	CACATTATTATGTAAACTATAATATACAATGTTGCCTATC AAGACAAACATATGCACTCTATGACATAGGCCACTAGTG GATCTG
rrm3::HIS3MX6	MB30	GAACAAGCTCAAAAGTCGAGAGATTTGTTCTTATAAGAC ATCCCGCGGATCCCCGGGTTAATTAA
	MB31	GAAAAGAAAACTTCAACTAGAGTATATGCATTTATTCGTT GCAAGGAATTCGAGCTCGTTTAAAC
sgs1::his5^{+}	MB32	TGTTGTATATATTTAAAAAATCATACACGTACACACAAGG CGGTACAGCTGAAGCTTCGTACGC
	MB33	GAATGGTGTCGTAGTTATAAGTAACACTATTTATTTTTCT ACTCTCGTATCCGGTGATCACCTAGAC
*prb1::*insert	KP321f	CAAACTTAAGAGTCCAATTAGCTTCATCGCCAATAAAAA AACAAACTAAACCTAATTCTAACA
	KP321r	TTGTAACCTCGAGACGCCTAAGGAAAGAAAAAGAAAAAA AAAAGCAGCTGAAATTTTTCTAAA

*The definitions of G4-I, G4-X, G-rich, and Non-G-rich are the same as in Tables S2 and 3.

B) Prokaryotic Pif1 cloning primers.

Species (helicase, accession #)	Oligo	Sequence (5'-3')*
Bacteroides sp. 2_1_16 (BacPif1, GG705209)	MB215	CGGGATCCATGGAAGATATGATTTTGACAGA AGAGATGCAAAAAATAATGAATCTC
	MB216	GATCCGCTCGAGATCTAACCGTTTACCATAA TAGTTACCTTCTGATTTGTATGCCC
Bdellovibrio bacteriovorus HD100 (BdePif1, BX842655)	MB211	CTGAAGATCTATGAATTCAGAGTCCAAATGC TATCGTTTTTATATTTGCTTCGC
	MB212	GATCCGCTCGAGAAGACCTTCAAACTGCTTA TAAAAATGCAAAACTTTTGGATCG
Campylobacter jejuni subsp. jejuni NCTC 11168 (CamPif1, AL111168)	MB196	CGGGATCCATGTTTGATAAACTAGAAAAAAT TTTAGCTTATGATAATGTTTTTTTAAGTG
	MB198	GATCCGCTCGAGGATTTGTTCTTGTATTTCG

		AGATCTAAAAAATTATGTTTTTT
Escherichia coli phage rv5 (rv5Pif1, DQ832317)	MB427	CGGGATCCGAAAAAGGGCAGTATGATGTAG GCACAGATGC
	MB428	GATCCGCTCGAGTACGTCCCCCTCTTCTGCT CTGGTTTC
Psychrobacter sp. PRwf-1 (PsyPif1, CP000713)	MB455	CAGTCGATTAATATGGGATCCAAACAAGCG ACCGCACTGG
	MB457	GATCCGCTCGAGATCAATAAAGACAAGCGC TAAGCGGATGG

*Restriction sites used to clone into the *Bam*HI and *Xho*I sites of the expression plasmids are underlined.

Table S7. Multiplex PCR primers.

Primer pair	**Sequences (5'->3')**	**Expected PCR product size (bp)**
PCM1 For	CGATGAAGGTTGATTACGAGC	615
PCM1 Internal Rev	GAAGGCTCCTATAAAGAACG	
IG SOM1 Rev	CGAGGTCACGGACACATATACC	
MB634	GACACGAAATTACAAAATGGAATATGTTC ATAGGGTAGACG	500
*Internal CIN8 Rev	GAAAATCGACATAATAAGAGTAGATTTCC	414
Internal CIN8 For	GATTTGCGATAGCGTCGCTGCC	
Internal NPR2 Rev2	CTTAGTTTAGAAATTTTGGCAATG	Rev2+Inside=340
Inside Hot Spot For	GAAAAGGATACAAAGGATATGAG	Rev2+Outside=451
Outside Hot Spot Rev	GTTTTCTTCGATTTGAAGGTGTTGG	
IG before CAN1 For	GAGTTTGCTAGATTCATAAAAGCC	241
IG before CAN1 Rev	CCGATAATGTCTGAGTTAGGTGAG	

*The PCR product generated by the *CIN8* primer pair was used as the probe for the Southern blots in Fig. 3.

Table S8. Plasmids

Name	Feature(s) of interest	Reference or source
pFA6a-Myc13-His3MX6	13xMyc, *HIS3*	[5]
pET28b-Pif1-His	*Saccharomyces cerevisiae PIF1*	[40]
pFB-MBP-SGS1-His	*S. cerevisiae SGS1*	[7]
pUC19+Bd3546 (for)	*Bdellovibrio bacteriovorus* Pif1	This study*
pMB116	N-terminal 4xStrepII tag, C-terminal 6xHis tag	This study
pMB131[a]	*Bacteroides* sp. 2_1_16 Pif1	This study
pMB142[a]	*B. bacteriovorus* Pif1	This study
pMB135[a]	*Campylobacter jejuni* Pif1	This study
pMB226[a]	*Escherichia coli* phage rv5 Pif1	This study
PMB241[a]	*Psychrobacter* sp. PRwf-1 Pif1	This study
pUG72	*URA3*	[4]
pFA6a-His3MX6	*HIS3*	[5]
pUG27	*his5*$^{+}$	[4]
pRS415	CEN *LEU2*	[1]
KP114[b]	G4 Chr I	This study
KP118[b]	G4 Chr X	This study
KP116[b]	GR Chr I	This study
KP117[b]	Chr VII	This study
pMB258	*CEN1*, *TRP1*, *RRM3* promoter, C-terminal 3xFLAG	This study
pMB282[c]	*S. cerevisiae PIF1*	This study
pMB307[c]	*CEN1*, *TRP1*, *PIF1* promoter, *PIF1*, C-terminal 3xFLAG	This study
pMB283[c]	*S. cerevisiae pif1*-K264A	This study
pMB274[c]	*S. cerevisiae RRM3*	This study
pMB272[c]	*Schizosaccharomyces pombe pfh1*$^{+}$	This study
pMB292[c]	*Homo sapiens PIF1*	This study
pMB270[c]	*Bacteroides* sp. 2_1_16 Pif1	This study
pMB288[c]	*Bacteroides* sp. 2_1_16 Pif1-KA	This study
pMB267[c]	*C. jejuni* Pif1	This study
pMB289[c]	*P.* sp. PRwf-1 Pif1	This study
pMB303[c]	*B. infantis* Pif1	This study
pMB304[c]	*Emiliana huxleyi* Virus 99B1 Pif1	This study
pMB305[c]	*B. bacteriovorus* Pif1	This study
pMB348[d]	*Schizosaccharomyces pombe* Pfh1	This study
pMB363[d]	*S. pombe* Pfh1-KA	This study

[a] Plasmid backbone = pMB116.
[b] Plasmid backbone = pRS415.
[c] Plasmid backbone = pRS258.
[d] Plasmid backbone = pRS424.
*A gift from Elizabeth Sockett (University of Nottingham).

References

1. Sikorski, R.S. & Hieter, P. A system of shuttle vectors and yeast host strains designed for efficient manipulation of DNA in *Saccharomyces cerevisiae*. *Genetics* **122**, 19-27 (1989).
2. Schulz, V.P. & Zakian, V.A. The *Saccharomyces PIF1* DNA helicase inhibits telomere elongation and *de novo* telomere formation. *Cell* **76**, 145-155 (1994).
3. Azvolinsky, A., Dunaway, S., Torres, J., Bessler, J. & Zakian, V.A. The *S. cerevisiae* Rrm3p DNA helicase moves with the replication fork and affects replication of all yeast chromosomes. *Genes Dev* **20**, 3104-3116 (2006).
4. Gueldener, U., Heinisch, J., Koehler, G.J., Voss, D. & Hegemann, J.H. A second set of loxP marker cassettes for Cre-mediated multiple gene knockouts in budding yeast. *Nucleic Acids Res* **30**, e23 (2002).
5. Longtine, M.S. et al. Additional modules for versatile and economical PCR-based gene deletion and modification in *Saccharomyces cerevisiae*. *Yeast* **14**, 953-961 (1998).
6. Boule, J.B. & Zakian, V.A. The yeast Pif1p DNA helicase preferentially unwinds RNA DNA substrates. *Nucleic Acids Res* **35**, 5809-5818 (2007).
7. Cejka, P. & Kowalczykowski, S.C. The full-length Saccharomyces cerevisiae Sgs1 protein is a vigorous DNA helicase that preferentially unwinds holliday junctions. *The Journal of biological chemistry* **285**, 8290-301 (2010).
8. Harmon, F.G. & Kowalczykowski, S.C. RecQ helicase, in concert with RecA and SSB proteins, initiates and disrupts DNA recombination. *Genes Dev* **12**, 1134-1144 (1998).
9. Studier, F.W. Protein production by auto-induction in high density shaking cultures. *Protein expression and purification* **41**, 207-34 (2005).
10. Capra, J.A., Paeschke, K., Singh, M. & Zakian, V.A. G-quadruplex DNA sequences are evolutionarily conserved and associated with distinct genomic features in Saccharomyces cerevisiae. *PLoS Comput Biol* **6**, e1000861 (2010).
11. Bachrati, C.Z. & Hickson, I.D. Analysis of the DNA unwinding activity of RecQ family helicases. *Methods Enzymol* **409**, 86-100 (2006).
12. Wong, I. & Lohman, T.M. A double-filter method for nitrocellulose-filter binding: application to protein-nucleic acid interactions. *Proc Natl Acad Sci U S A* **90**, 5428-32 (1993).
13. Brosh, R.M., Jr., Opresko, P.L. & Bohr, V.A. Enzymatic mechanism of the WRN helicase/nuclease. *Methods in enzymology* **409**, 52-85 (2006).
14. Putnam, C.D. & Kolodner, R.D. Determination of gross chromosomal rearrangement rates. *Cold Spring Harbor protocols* **2010**, pdb prot5492 (2010).
15. Hall, B.M., Ma, C.X., Liang, P. & Singh, K.K. Fluctuation analysis CalculatOR: a web tool for the determination of mutation rate using Luria-Delbruck fluctuation analysis. *Bioinformatics* **25**, 1564-5 (2009).
16. Kushnirov, V.V. Rapid and reliable protein extraction from yeast. *Yeast* **16**, 857-60 (2000).
17. Runge, K.W. & Zakian, V.A. Introduction of extra telomeric DNA sequences into *Saccharomyces cerevisiae* results in telomere elongation. *Mol. Cell. Biol.* **9**, 1488-1497 (1989).
18. Azvolinsky, A., Giresi, P., Lieb, J. & Zakian, V. Highly transcribed RNA polymerase II genes are impediments to replication fork progression in Saccharomyces cerevisiae. *Mol Cell* **34**, 722-734 (2009).
19. Paeschke, K., Capra, J.A. & Zakian, V.A. DNA Replication through G-Quadruplex Motifs Is Promoted by the Saccharomyces cerevisiae Pif1 DNA Helicase. *Cell* **145**, 678-91 (2011).
20. Livak, K.J. & Schmittgen, T.D. Analysis of relative gene expression data using real-time quantitative PCR and the 2(-Delta Delta C(T)) Method. *Methods* **25**, 402-8 (2001).

21. Law, M.J. et al. ATR-X syndrome protein targets tandem repeats and influences allele-specific expression in a size-dependent manner. *Cell* **143**, 367-78 (2010).
22. Mohaghegh, P., Karow, J.K., Brosh Jr, R.M., Jr., Bohr, V.A. & Hickson, I.D. The Bloom's and Werner's syndrome proteins are DNA structure-specific helicases. *Nucleic Acids Res* **29**, 2843-2849 (2001).
23. Sun, H., Karow, J., Hickson, I. & Maizels, N. The Bloom's Syndrome Helicase Unwinds G4 DNA. *J. Biol. Chem.* **273**, 27587-27592 (1998).
24. Popuri, V. et al. The Human RecQ helicases, BLM and RECQ1, display distinct DNA substrate specificities. *J Biol Chem* **283**, 17766-17776 (2008).
25. Huber, M.D., Lee, D.C. & Maizels, N. G4 DNA unwinding by BLM and Sgs1p: substrate specificity and substrate-specific inhibition. *Nucl Acids Res.* **30**, 3954-3961 (2002).
26. Wu, Y., Sommers, J.A., Khan, I., de Winter, J.P. & Brosh, R.M., Jr. Biochemical characterization of Warsaw breakage syndrome helicase. *The Journal of biological chemistry* **287**, 1007-21 (2012).
27. Chakraborty, P. & Grosse, F. Human DHX9 helicase preferentially unwinds RNA-containing displacement loops (R-loops) and G-quadruplexes. *DNA repair* **10**, 654-65 (2011).
28. Masuda-Sasa, T., Polaczek, P., Peng, X.P., Chen, L. & Campbell, J.L. Processing of G4 DNA by Dna2 helicase/nuclease and replication protein A (RPA) provides insights into the mechanism of Dna2/RPA substrate recognition. *J Biol Chem* **283**, 24359-24373 (2008).
29. Gonzalez, V., Guo, K., Hurley, L. & Sun, D. Identification and characterization of nucleolin as a c-myc G-quadruplex-binding protein. *The Journal of biological chemistry* **284**, 23622-35 (2009).
30. London, T.B. et al. FANCJ is a structure-specific DNA helicase associated with the maintenance of genomic G/C tracts. *J Biol Chem* **283**, 36132-36139 (2008).
31. Baran, N., Pucshansky, L., Marco, Y., Benjamin, S. & Manor, H. The SV40 large T-antigen helicase can unwind four stranded DNA structures linked by G-quartets. *Nucleic acids research* **25**, 297-303 (1997).
32. Tuesuwan, B. et al. Simian virus 40 large T-antigen G-quadruplex DNA helicase inhibition by G-quadruplex DNA-interactive agents. *Biochemistry* **47**, 1896-909 (2008).
33. Ribeyre, C. et al. The yeast Pif1 helicase prevents genomic instability caused by G-quadruplex-forming CEB1 sequences *in vivo*. *PLoS Genet* **5**, e1000475 (2009).
34. Sanders, C.M. Human Pif1 helicase is a G-quadruplex DNA binding protein with G-quadruplex DNA unwinding activity. *Biochem J* (2010).
35. Wu, X. & Maizels, N. Substrate-specific inhibition of RecQ helicase. *Nucleic acids research* **29**, 1765-71 (2001).
36. Giri, B. et al. G4 resolvase 1 tightly binds and unwinds unimolecular G4-DNA. *Nucleic acids research* **39**, 7161-78 (2011).
37. Lattmann, S., Giri, B., Vaughn, J.P., Akman, S.A. & Nagamine, Y. Role of the amino terminal RHAU-specific motif in the recognition and resolution of guanine quadruplex-RNA by the DEAH-box RNA helicase RHAU. *Nucleic acids research* **38**, 6219-33 (2010).
38. Shum, K.T. & Tanner, J.A. Differential inhibitory activities and stabilisation of DNA aptamers against the SARS coronavirus helicase. *Chembiochem : a European journal of chemical biology* **9**, 3037-45 (2008).
39. Fry, M. & Loeb, L.A. Human Werner syndrome DNA helicase unwinds tetrahelical structures of the fragile X syndrome repeat sequence d(CGG)n. *J. Biol. Chem.* **274**, 12797-12802 (1999).
40. Boule, J., Vega, L. & Zakian, V. The Yeast Pif1p helicase removes telomerase from DNA. *Nature* **438**, 57-61 (2005).